1 Introduction

Life, as we know it, is based on the capability of problem solving [Popp 96]. The problems or questions studied by natural scientists today are usually highly specialized. This is because the solution of a problem typically opens the view on deeper problems that have not been realized before. Thanks to the strong methodology of the natural sciences [Popp 05] this process of basic research increases our knowledge about the nature or better the reality, and gives the impulses for new technological applications. A basic research field that has led to many important technological applications, e.g. of transistors and semiconductors, is solid-state physics, which forms the theoretical foundation of materials science. The topics covered in this thesis can be allocated to two branches of solid-state physics: thermoelectrics and thermal spintronics or spin caloritronics.

Research in the field of **thermoelectrics** explores the non-equilibrium transport of charge and heat in conducting materials and devices [Nola 01]. The basic thermoelectric phenomena, which are the Seebeck effect and the Peltier effect (see Table 1.1), were discovered already in the 19th century. It was soon recognized that these effects are useful for applications, such as thermometry, refrigeration, and power generation. With the rise of quantum mechanics in the first half of the 20th century the understanding of thermoelectricity increased significantly, so that the most promising natural materials for thermoelectric applications had been figured out before 1960. These are alloys of the three compounds Bi_2Te_3, Sb_2Te_3, and Bi_2Se_3, which are semiconductors with rather small bandgaps ($E_g \approx 0.1$ eV) and carrier concentrations of the order of 1×10^{19} cm^{-3} at room temperature. In the 30 years that followed, thermoelectricity had found some small but important applications, e.g. in radioisotope-thermoelectric generators that supply thermal and electrical power during space missions [Furl 99]. However, the efficiency of thermoelectric refrigerators remained too small for making them competitive with conventional cooling devices. Within the last 20 years, new strategies have been developed for enhancing the thermoelectric efficiency, for example by synthesizing materials with greater chemical complexity [Snyd 08], or by nanostructuring of thermoelectric materials [Dres 07, Minn 09, Vine 10, Pich 10, Kana 10]. The latter approach endeavors to make use of quantum confinement effects that can modify the energy dependence of the density of electronic states and can increase their effective band gap [Pich 10]. Furthermore, it is possible to reduce the phonon contributions to the thermal conductivity by nanostructuring [Kana 10]. A low thermal conductivity is crucial for thermal refrigeration to maintain the temperature gradient during cooling, but can be less important in the context of waste-heat recovery using thermoelectric generators [Nard 11]. Although the great promises of nanotechnology have unfortunately not materialized to date, it is very likely that the recent interest in waste-heat recovery [Rowe 06], as well as new applications, such as chip-scale thermoelectric cooling of transistors [Chow 09], may lead to an increased demand for thermoelectric devices. In recent years renewed interest in thermoelectric materials has been initiated by the prediction and subsequent demonstrations that many established thermoelectric materials (e.g. Bi_xSb_{1-x}, Bi_2Te_3, Bi_2Se_3) can exhibit signatures of topological insulators [Moor 10].

Some of the basic non-equilibrium transport phenomena are listed in Table 1.1. These phenomena may be separated into thermoelectric effects (Seebeck, Peltier, Thomson), galvanomagnetic effects (Hall, Ettingshausen), and thermomagnetic effects (Nernst, Righi-Leduc). Furthermore, in ferromagnetic conductors there are magnetoresistive effects, such as the anisotropic magnetoresistance effect and the giant magnetoresistance effect, as well as so-called anomalous (planar) effects that are observed if the magnetization is aligned perpendicular (parallel) to the currents, such as the anomalous- (planar-) Hall effect and the anomalous- (planar-) Nernst effect. The physical mechanisms behind the anomalous and planar effects are completely different from the respective 'normal' effects [Naga 10]. The common grounds that may justify the shared names are the related experimental geometries.

The anomalous and planar effects that involve temperature gradients, as well as the thermal and thermoelectric analogues of the magnetoresistive effects, such as the giant magnetothermal resistance effect and the giant magneto-Seebeck effect, may be counted to the new field of **thermal spintronics** or **spin caloritronics**, which explores non-equilibrium transport phenomena of spin, charge, and heat transport in ferromagnetic materials and ferromagnetic/non-magnetic hybrid structures [Baue 10, Baue 12]. Considering the spin degree of freedom further increases the zoo of non-equilibrium transport phenomena. Effects that are denoted by 'spin dependent', such as the spin-dependent Seebeck effect and the spin-dependent Peltier effect, rely on spin currents carried by spin polarized conduction electrons, while those denoted by 'spin', such as the spin-Hall effect, the spin-Nernst effect, and the spin-Seebeck effect, are thought to be based on pure spin currents. Another effect that involves pure spin currents is the thermal spin transfer torque [Hata 07, Yu 10]. Spin currents are a major issue in the field of spintronics. This research area has made a tremendous impact with the commercialization of magnetic hard disk drives that use spin-valves for data reading, and is coming up with many future applications [Bade 10]. Particular attention on thermal spintronics has been triggered by the spin-Seebeck effect − the evolution of a transverse voltage in a paramagnetic metal that is in thermal contact with the spin-Seebeck material under the influence of a temperature gradient and external magnetic fields. To explain the spin-Seebeck voltage it is assumed that the temperature gradient is associated with a spin current, which flows into the paramagnetic metal and causes a voltage due to the inverse spin-Hall effect [Uchi 08]. This interpretation suggests that pure spin currents may propagate over macroscopic length scales. Soon later the spin-Seebeck effect was also found, e.g., in electrically insulating yttrium iron garnet [Uchi 10] and even in a non-magnetic semiconductor [Jawo 12]. Perhaps over-motivated by the technological importance of spin currents, serious efforts have been undertaken to find a theory that explains the physical origin of the presupposed spin current in the spin-Seebeck effect [Xiao 10, Adac 13], although this spin current has only been measured indirectly. There is an ongoing debate about this topic and it could be possible that the spin-Seebeck effect will be explained in the light of a much simpler theory. This view is supported by the recent work of Avery *et al.*, who explained the signatures of the spin-Seebeck effect in their experiments in terms of the planar-Nernst effect [Aver 12].

So much for the problem situations of thermoelectrics and thermal spintronics. It is the objective of this thesis to make some small contributions to these research fields. The thesis is organized as follows:

Chapter 2 provides theoretical foundations that may be required for the discussion of our experiments. Chapter 3 demonstrates a synthesis route to nearly intrinsic Bi_2Te_3 nanowires, discusses the measuring microdevice used for determining the Seebeck coefficient, and presents a structural and compositional analysis as well as thermoelectric transport measurements on individual Bi_2Te_3 nanowires. Chapter 4 deals with the 3ω method, which is a prevalent measuring technique of thermal properties of bulk materials, thin films and nanowires. The concept of the 3ω method is revisited for voltage-driven measurement setups. Chapter 5 focuses on the electrical and thermal transport in individual Ni nanowires. A simple model is proposed to describe a new effect, the anisotropic magnetothermal resistance effect. Experimental results on this effect are presented. Chapter 6 is concerned with the electrical and thermal transport in Co/Cu multilayers. The Wiedemann-Franz law is revisited, which is complemented by measurements of the giant magnetoresistance effect and the giant magnetothermal resistance effect. Chapter 7 closes the thesis with a conclusion that summarizes our main results and suggests further experiments. In Appendix A our review article "Thermoelectric Nanostructures: From Physical Model Systems towards Nanograined Composites" is reprinted, which may by of interest for the reader in connection with Chapter 4. In Appendix B a philosophical article is reprinted. In particular natural scientists, who often get lost in highly specialized technical problems, should show an open-mindedness toward philosophical problems, perhaps in particular toward those related to the scientific method and the history of science (compare Ref. [Lder 12]).

Table 1.1: Basic non-equilibrium transport phenomena [Nola 01]. **E**: Electric field, T: Temperature, **q**: Heat current density, **j**: Current density, p: Power density, ρ: Resistivity, H_z: Magnetic field strength.

Phenomenon	Phenomenological description	Formula
Seebeck effect	A temperature gradient imposed on a conductor generates a diffusion current. Under open circuit conditions an electric field acting against the temperature gradient develops and finally balances the diffusion current.	$\mathbf{E} = S\,\nabla T$; S: Seebeck coefficient.
Peltier effect	A voltage imposed on a conductor generates a charge current that is associated with a heat current. The change of the total energy flow at a junction of two conductors is accompanied by evolution of heat at the junction.	$\mathbf{q} = \Pi\,\mathbf{j}$; Π: Peltier coefficient.
Thomson effect	A current traversing a temperature gradient in a conductor is accompanied by evolution of Thomson heat in addition to the Joule heat.	$p = \rho\,\mathbf{j}^2 - \mu\,\mathbf{j}\nabla T$; μ: Thomson coefficient.
Hall effect	A current-carrying conductor placed in a transverse magnetic field develops an electric field perpendicular to the current and magnetic field directions.	$E_y = R_\mathrm{H} H_z j_x$; R_H: Hall coefficient.
Ettingshausen effect	A current-carrying conductor placed in a transverse magnetic field develops a temperature gradient perpendicular to the current and magnetic field directions.	$\frac{dT}{dx} = R_\mathrm{E} H_z j_x$; R_E: Ettingshausen coefficient.
Nernst effect	A heat current carrying conductor placed in a transverse magnetic field develops an electric field perpendicular to the heat current and magnetic-field directions.	$E_y = R_\mathrm{N} H_z \frac{dT}{dx}$; R_N: Nernst coefficient.
Righi-Leduc effect	A heat current carrying conductor placed in a transverse magnetic field develops a temperature gradient perpendicular to the current and magnetic field directions.	$\frac{dT}{dy} = R_\mathrm{RL} H_z \frac{dT}{dx}$; R_RL: Righi-Leduc coefficient.

2 Theoretical Foundations

This chapter deals with the basic physics relevant for this thesis. The main focus is on electronic transport phenomena in conducting materials, in particular ferromagnets. Section 2.1 briefly recapitulates the main magnetic interactions in electron systems. Section 2.2 introduces the Boltzmann-transport theory, which is used in Sec. 2.3 to quickly arrive at the basic thermoelectric effects. Since it is a major issue of thermoelectrics to find strategies for enhancing the efficiency of thermoelectric devices, Sec. 2.4 introduces the thermoelectric figure of merit. In Sec. 2.5, a discussion of the basic bulk optimization strategies that are based on tuning of the carrier concentration and looking for high carrier mobilities follows. Section 2.6 briefly summarizes the dominant scattering mechanisms of electrons. The two subsequent sections introduce two famous laws in solid state physics: the Matthiessen law in Section 2.7 and the Wiedemann-Franz law in Sec. 2.8. Coming back to magnetism, Sec. 2.9 discusses the peculiarities of electronic transport in ferromagnets and Sec. 2.10 introduces the anisotropic magnetoresistance effect. Section 2.11 addresses the spin-dependent diffusive transport theory that leads to the concepts of spin- and spin-heat-accumulation, followed by a discussion of the giant magnetoresistance effect in Sec. 2.12. The last section of this chapter deals with classical size effects, which are always present in nanostructures, and quantum confinement effects, which can play a significant role in nanostructures.

2.1 Magnetism

There are three main magnetic interactions in electron systems [Sthr 06]: The exchange interaction that is responsible for the alignment of spins, the spin-orbit interaction that creates orbital magnetism and couples the spin system to the lattice, and the Zeeman interaction that enables us to manipulate the alignment of magnetic moments.

2.1.1 Exchange Interaction

The exchange interaction is a quantum-mechanical effect between identical particles. It arises from the symmetrization postulate. According to this postulate, the total wavefunction of an electron system is antisymmetric under exchange of any two electrons. Due to the antisymmetric wavefunction the Coulomb potential between the electrons in the system acts as if it was spin-dependent [Gasi 02]. The resulting change of the expectation value of the energy favors either parallel or antiparallel spins. The fact that the exchange interaction arises from the wavefunctions imposes big challenges on the theoretical description, in particular for macroscopic systems. Therefore, one often uses a model Hamiltonian, e.g. the Heisenberg Hamiltonian or the Hubbard Hamiltonian, which are designed to give suitable results for well-known problems, in combination with one-particle wavefunctions [Sthr 06]. One distinguishes several forms of exchange. Important examples are given in the following.

Direct exchange is due to direct overlap of the wavefunctions considered for exchange. In He atoms direct exchange between the two electrons favors parallel spins. The exchange energy split between triplet and singlet states of excited He atoms is observable

in the spectrum of He. In H_2 molecules direct exchange between the two electrons favors antiparallel spins. Due to the wavefunction overlap between the H^+ ions a bonding orbital is formed. In that way, the exchange interaction gives a physical explanation of the covalent chemical bond.

Indirect exchange between two magnetic atoms can be mediated by a nonmagnetic atom. It leads to antiferromagnetic coupling and occurs for example in transition metal oxides, such as NiO. This kind of indirect exchange is called superexchange, because it extends the short-ranging direct exchange interaction to longer distances. Another important example for indirect exchange is the RKKY interaction[1] that describes the exchange over the distance between two localized magnetic electrons mediated by conduction electrons. Scattering of conduction electrons at the localized magnetic electrons generates spin-density waves in the itinerant electron system that screen the disturbing localized magnetic moment. This leads to an oscillatory behavior of the RKKY-exchange interaction. Depending on the distance between the localized magnetic electrons, their magnetic coupling can be ferromagnetic or antiferromagnetic. The RKKY interaction works over relatively large distances of a few nanometers. It can be used to couple magnetic layers that are separated by a nonmagnetic spacer layer. As discussed in Sec. 2.12, this possibility is of highest practical interest.

Itinerant exchange means exchange between itinerant electrons. In the ferromagnetic transition metals Fe, Co, and Ni, the exchange interaction causes a spontaneous magnetization, i.e. a parallel alignment of spins over macroscopic regions or domains, even in the absence of external magnetic fields. The main source of the spontaneous magnetization in transition metals are the spin moments of partly occupied $3d$ states at the Fermi energy that generate a sizeable magnetization at room temperature. A general theory of ferromagnetic transition metals should describe simultaneously the characteristic electron correlation effects that lead to the spontaneous magnetization, as well as the electronic transport properties predicted by band theories [Sthr 06].[2] The formulation of such a theory is a topic of contemporary research in magnetism. Instead of such a theory, a widely supported description is given by the Stoner model that is based on band theory [Sthr 06]. This model assumes that an exchange interaction of $3d$ electrons generates an exchange-energy splitting of the $3d$ bands. As the $3d$ bands are not fully occupied, the exchange splitting increases the number of electrons in the energetically favored band, and vice versa. The spin-polarized $3d$ bands give rise to a spontaneous magnetization that is determined by the difference of the occupation numbers of both bands. Due to the filling of the bands up to the Fermi surface the magnetic moment per atom is a noninteger multiple of the Bohr magneton. Electrons with spin orientation antiparallel to the magnetization vector are called majority-spin electrons. The others are called minority-spin electrons. In Fig. 2.1, the Stoner model is illustrated for Ni. The exchange interaction is the strongest among the three magnetic interactions, because it arises from the Coulomb interaction. In the $3d$ transition metals, the exchange energy is of the order of 1 eV.

---

[1]Named after the scientists involved in the discovery of this effect: Ruderman, Kittel, Kasuya, and Yosida.

[2]The behavior of electrons in solids has largely remained a mystery. One distinguishes two important concepts: localized or correlated and independent, delocalized, itinerant, or band-like electron behavior [Sthr 06]. Correlated electrons remain localized on different atomic sites due to dominating Coulomb repulsion, whereas the wavefunctions of independent electrons in a solid are spread over the entire crystal. Such delocalized electrons are itinerant and can be well described by band-theoretical models.
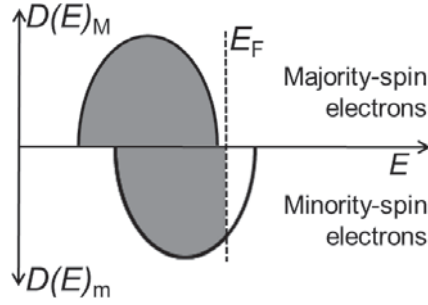
Figure 2.1: Illustration of the spin-polarized $3d$ band of Ni in the Stoner model. Minority spins point in the direction of the spontaneous magnetization. The bands are separated due to the exchange energy splitting. Filled electron states below the Fermi energy E_F are indicated by the shaded area. This figure is based on Fig. 7.6 in Ref. [Sthr 06].

2.1.2 Spin-Orbit Interaction

The spin $\mathbf{S}$ of an electron couples with the orbital angular momentum $\mathbf{L}$ of the electron to the total angular momentum $\mathbf{J} = \mathbf{S} + \mathbf{L}$. This effect is described by the spin-orbit Hamiltonian H_so, which follows from the relativistic Dirac equation [Sthr 06]:

$$H_\mathrm{so} = \xi\, \mathbf{L} \cdot \mathbf{S}, \tag{2.1}$$

where ξ is the spin orbit coupling constant. In a crystal, electron orbitals are linked to the lattice due to bonding with adjacent atoms, i.e. the orbital angular momentum favors certain crystallographic directions. This anisotropy combined with the spin-orbit interaction leads to the magnetocrystalline anisotropy in ferromagnetic materials. On the other hand, the presence of a spontaneous magnetization coupled to the lattice breaks the time-reversal symmetry and allows for a net orbital magnetization. Applied to $3d$ orbitals of ferromagnetic transition metals with an energy splitting due to a ligand field of cubic symmetry, the spin-orbit interaction generates mixing of states with the same spin and mixing of states with opposite spin [Sthr 06]. It turns out that this intermixing effect is anisotropic. We come back to this point in Sec. 2.10, where the anisotropic magnetoresistance is discussed. The spin-orbit interaction energy in the $3d$ transition metals is of the order of 10 to 100 meV.

2.1.3 Zeeman Interaction

The Zeeman interaction describes the coupling of angular momentum to an external magnetic field $\mathbf{H}$. The total angular momentum $\mathbf{J} = \mathbf{L} + \mathbf{S}$ generates a magnetic moment $\mathbf{m} = -\frac{\mu_\mathrm{B}}{\hbar}(\mathbf{L} + 2\mathbf{S})$. The Zeeman Hamiltonian is given by [Sthr 06]

$$H_\mathrm{ZI} = \frac{\mu_\mathrm{B}}{\hbar}(\mathbf{L} + 2\mathbf{S}) \cdot \mathbf{H}. \tag{2.2}$$

In atoms, the Zeeman interaction lifts the degeneracy of electronic states. In ferromagnetic materials, the Zeeman interaction allows for the alignment of magnetic domains by applying magnetic fields.

2.2 Boltzmann Equation and Relaxation-Time Approximation

A system of noninteracting identical fermions can be described using Fermi-Dirac statistics. Application of Fermi-Dirac statistics to electrons in metals is known as the Sommerfeld theory of metals. The average number of electrons in a single-particle state of energy E at equilibrium is described by the Fermi-Dirac function

$$f_0(E,T) = \frac{1}{e^{(E-\zeta)/k_\mathrm{B}T} + 1}, \tag{2.3}$$

where ζ is the chemical potential, which at $T = 0$ is equal to the Fermi energy. Within the semi-classical transport theory, the nonequilibrium distribution function f is defined to depend on the wave vector $\mathbf{k}$, the spatial coordinate $\mathbf{r}$, and the time t. To justify the assumption of a classical position-momentum space, it is assumed that the chemical potential and the temperature vary over a scale that is large compared to atomic dimensions. The differential equation for $f(\mathbf{k}, \mathbf{r}, t)$ is the Boltzmann equation, a continuity equation for particle flow:

$$\frac{df(\mathbf{k},\mathbf{r},t)}{dt} = \frac{\partial f(\mathbf{k},\mathbf{r},t)}{\partial t} + \nabla_r f(\mathbf{k},\mathbf{r},t)\frac{d\mathbf{r}}{dt} + \nabla_k f(\mathbf{k},\mathbf{r},t)\frac{d\mathbf{k}}{dt} = \left(\frac{\partial f(\mathbf{k},\mathbf{r},t)}{\partial t}\right)_{\mathrm{coll}}, \tag{2.4}$$

where the collision term on the right hand side contains the information about the microscopic scattering mechanisms. The linearized Boltzmann equation for steady-state distribution functions ($\frac{\partial f}{\partial t} = 0$) is obtained by replacing f with f_0 in the left hand side of Eq. (2.4). This is reasonable for weak external fields, so that the system is not too far from equilibrium. The simplest approximation of the right hand side is the relaxation time approximation. For this approach it is assumed that the collision term, which is responsible for the system to approach thermal equilibrium, is proportional to the deviation of the distribution function from its equilibrium value. The linearized Boltzmann equation in the relaxation time approximation then reads [Uher 04]:

$$\left(\frac{df_0(\mathbf{k})}{dE}\right)\left[\frac{E(\mathbf{k}) - \zeta}{T}\nabla_r T + \nabla_r\zeta - e\mathbf{E}\right]\mathbf{v} = -\frac{f(\mathbf{k},\mathbf{r}) - f_0(\mathbf{k})}{\tau(\mathbf{k})}, \tag{2.5}$$

where $\tau(\mathbf{k})$ is the relaxation time and $\mathbf{E} = \frac{\hbar}{e}\frac{d\mathbf{k}}{dt}$ the electrostatic field.[3] The validity of the relaxation-time approximation is a critical issue [Ashc 76]. Inelastic scattering processes for example can be very effective in relaxing a thermal current without degrading an electric current. As a consequence of the relaxation-time approximation, τ would be different for heat- and charge-currents. Consequently, the interpretation of the relaxation time as a measure of the time between two collisions is not valid anymore. Before we come back to this point in Sec. 2.8, Eq. (2.5) is used to define the current densities that are caused by an electric field and a temperature gradient.

---

[3]The effective field that drives the current is given by $\epsilon = \mathbf{E} - \nabla_r\zeta/e = -\nabla_r(\varphi + \zeta/e) \equiv -\nabla_r\Phi/e$, where $\Phi = \zeta + e\varphi$ is the electrochemical potential. Throughout the text the elementary charge e is defined as a parameter (compare Table 0.1), i.e. the charge of an electron is $-e$.

2.3 Thermoelectric Effects

The nonequilibrium distribution described by Eq. (2.5) results in nonvanishing charge- and heat-current densities that are given by

$$\mathbf{j}(\mathbf{r}) = \frac{2e}{V} \sum_{\mathbf{k}} \mathbf{v}(\mathbf{k}) f(\mathbf{k,r}), \qquad (2.6)$$

and

$$\mathbf{q}(\mathbf{r}) = \frac{2}{V} \sum_{\mathbf{k}} \mathbf{v}(\mathbf{k})(E(\mathbf{k}) - \zeta) f(\mathbf{k,r}). \qquad (2.7)$$

Substituting Eq. (2.5) into Eqs. (2.6) and (2.7) results in a linear relation between the external fields and their associated currents[4] [Uher 04],

$$\mathbf{j}(\mathbf{r}) = e^2 K_0 \mathbf{E} + \frac{eK_1}{T}(-\nabla_r T), \qquad (2.8)$$

$$\mathbf{q}(\mathbf{r}) = eK_1 \mathbf{E} + \frac{K_2}{T}(-\nabla_r T), \qquad (2.9)$$

where the transport coefficients K_n are in general tensors:

$$K_{n,(i,j)} = \frac{2}{V} \sum_{\mathbf{k}} v_i(\mathbf{k}) v_j(\mathbf{k}) [E(\mathbf{k}) - \zeta]^n \tau(\mathbf{k}) \left(-\frac{df_0(\mathbf{k})}{dE} \right). \qquad (2.10)$$

For isotropic materials the tensors reduce to scalars. Assuming zero temperature gradient, Eq. (2.8) reduces to the Ohm law:

$$\mathbf{j} = e^2 K_0 \mathbf{E} \equiv \sigma \mathbf{E}, \qquad (2.11)$$

where σ is the electrical conductivity. Under open-circuit conditions ($\mathbf{j} = 0$), Eq. (2.8) describes the generation of an electric field by a temperature gradient:

$$\mathbf{E} = \frac{K_0^{-1} K_1}{eT} \nabla_r T \equiv S \ \nabla_r T, \qquad (2.12)$$

where S is the Seebeck coefficient. An important application of this so-called Seebeck effect is the thermocouple (see Fig. 2.2). The two legs of a thermocouple consist of two materials with different Seebeck coefficients, S_A and S_B. According to Eq. (2.12), the temperature difference across the legs of the thermocouple generates the voltage

$$U_{ac} = \int_a^b S_A \nabla_r T d\mathbf{r} + \int_b^c S_B \nabla_r T d\mathbf{r} = (S_A - S_B)(T_2 - T_1), \qquad (2.13)$$

which can be used for temperature measurements (compare Fig. 2.2). In the absence of a temperature gradient, it follows from Eqs. (2.8) and (2.9) that the heat current generated by a voltage is proportional to the charge current:

$$\mathbf{q} = \frac{K_1 K_0^{-1}}{e} \mathbf{j} \equiv \Pi \ \mathbf{j}, \qquad (2.14)$$

---

[4]In metals the chemical potential is not affected by the transport process and can be assumed constant, i.e. $\nabla_r \zeta = 0$. This is because of their large carrier concentrations.
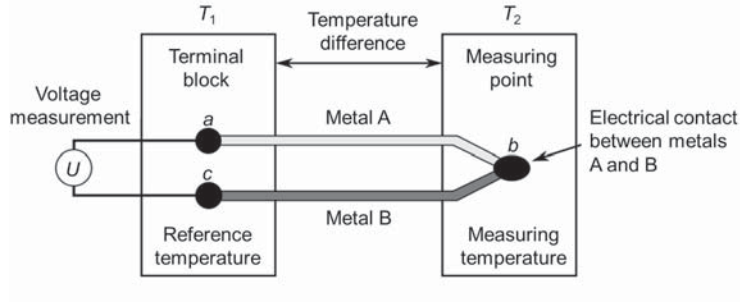
Figure 2.2: Basic thermoelement that can be used to measure temperatures. The figure is based on a public file [wwwc 08].

where Π is called the Peltier coefficient. A current that flows through a thermocouple is accompanied by the evolution of heat at the junction of the two materials. This so-called Peltier effect has its application in thermoelectric refrigeration.

The thermal conductivity is typically measured under open-circuit conditions ($\mathbf{j} = 0$). Then, substituting Eq. (2.12) into Eq. (2.9) yields

$$\mathbf{q} = \frac{K_2 - K_1 K_0^{-1} K_1}{T}(-\nabla_r T) \equiv \kappa(-\nabla_r T), \qquad (2.15)$$

where κ is the electronic thermal conductivity. For metals, the term $K_1 K_0^{-1} K_1 \ll K_2$ and can therefore be neglected in Eq. (2.15).

Using Eqs. (2.8) and (2.9) the entropy current density $\mathbf{s} = \mathbf{q}/T$ can be expressed in terms of the current density and the temperature gradient:

$$\mathbf{s} = \frac{K_1 K_0^{-1}}{eT}\mathbf{j} + \frac{K_2 - K_1 K_0^{-1} K_1}{T^2}(-\nabla_r T). \qquad (2.16)$$

According to this equation, the Seebeck coefficient defined in Eq. (2.12) is equal to the entropy per charge carried by a current in a conductor.

2.4 Thermoelectric Figure of Merit

It can be shown that both the power generation efficiency and the cooling coefficient of performance of a thermoelement (see Fig. 2.2) are maximized by maximizing the figure of merit [Nola 01]

$$ZT = \frac{(S_A - S_B)^2}{\left(\sqrt{\kappa_A \rho_A} + \sqrt{\kappa_B \rho_B}\right)^2}T, \qquad (2.17)$$

where $\rho = 1/\sigma$ is the electrical resistivity. In typical applications, the absolute thermoelectric properties of the two materials are similar, and Z approximately equals the average of the individual figures of merit. Multiplied with the temperature, the dimensionless individual figure of merit is defined to be

$$zT = \frac{S^2}{\kappa \rho}T = \frac{S^2 \sigma}{\kappa}T. \qquad (2.18)$$